

# Electronically Switchable and Tunable Coplanar Waveguide–Slotline Band-Pass Filters

Yong-Hui Shu, Julio A. Navarro, and Kai Chang, *Fellow, IEEE*

**Abstract**—A novel coplanar waveguide (CPW) slotline band-pass filter has been developed. The circuit allows planar integration of active and passive semiconductor devices both in series and in shunt. To test the filter, a new microstrip to slotline transition was designed and two of these transitions exhibited an insertion loss of less than 1.0 dB over the 2.0 to 4.0 GHz range. A three-section CPW–slotline band-pass filter demonstrated an insertion loss of less than 0.2 dB over the passband centered at 2.9 GHz. A three-section CPW–slotline switchable band-pass filter integrated with three p-i-n diodes was developed with a 0.7 dB insertion loss in the passband when the p-i-n diodes are off and 25.0 dB isolation across the entire band when the p-i-n diodes are on. A three-section CPW–slotline varactor-tunable filter integrated with three varactor diodes was demonstrated with a 2.0 dB insertion loss and over 20% electronic tuning range. Simple transmission line circuit models were used to optimize the design.

## I. INTRODUCTION

THERE is an increasing demand to use microwave and millimeter-wave hybrid and monolithic integrated circuits for many system applications. Because of their planar nature, these circuits offer cost, weight, reliability, and reproducibility advantages when combined with photolithographic techniques. Microstrip has been the main transmission line used in microwave circuit design, partly because of the vast amount of design information available. Although semiconductor devices can be readily integrated in series, shunt devices must be mounted by drilling through the substrate. Drilling adds cost and discontinuities which make the design more difficult and degrade the performance, especially at millimeter-wave frequencies. Furthermore, the microstrip impedance and guided-wavelength characteristics are very sensitive to substrate thickness, which further increases design problems at higher frequencies.

Coplanar waveguide (CPW) is an alternative transmission line that is truly planar and allows easy series and shunt device mounting. CPW is not very sensitive to substrate thickness and allows a wide range of impedance values on relatively thick substrates. The radiation loss in the CPW odd mode is low for an open transmission line. These charac-

Manuscript received June 12, 1990; revised October 3, 1990. This work was supported in part by the U.S. Army Research Office and the Texas Higher Education Coordinating Board's Advanced Technology Program.

Y.-H. Shu was with the Department of Electrical Engineering, Texas A&M University, College Station, TX. He is now with the Epsilon Lambda Electronics Corporation, Geneva, IL 60134.

J. A. Navarro and K. Chang are with the Department of Electrical Engineering, Texas A&M University, College Station, TX 77843-3128.

IEEE Log Number 9041958.



Fig. 1. Cross-sectional view of microstrip line, slotline, and coplanar waveguide.

teristics make CPW important for millimeter-wave circuits and have aroused considerable interest in microwave and millimeter-wave integrated circuit design [1]–[3]. Although several papers [4]–[6] analyze the characteristics and advantages of CPW, there are only a limited number of CPW components available for circuit design. These components include directional couplers [6]–[7], mixers [8], [9], diplexers [10], [11], and end-coupled resonant CPW filters [12]. This paper describes the integration of microstrip, slotline, and CPW to create a novel CPW slotline band-pass filter and a new microstrip-to-slotline transition.

Fig. 1 shows a cross-sectional view of each of these transmission lines. The filter uses CPW resonators interconnected via slotline. The filter is planar and allows easy series and shunt device mounting. Transmission line models were developed to design the filters. To test the filters, a new microstrip-to-slotline transition was developed. This transition is unique and differs from previous transitions [13] due to the advantage of providing dc blocks required for device biasing and low-pass filters to reduce the transition loss.

A pair of microstrip-to-slotline transitions was developed with a 1.0 dB loss throughout the 2.0 to 4.0 GHz band. A three-section CPW–slotline filter was developed with less than 0.2 dB insertion loss in the passband and over 30.0 dB isolation in the stopbands. Integrating three p-i-n diodes in the three-section filter created a switchable filter. When the p-i-n diodes were reversed-biased, the switchable filter exhibited a 0.7 dB insertion loss in the passband and over 30.0 dB in the stop bands. When the p-i-n diodes were forward-biased, the switchable filter exhibited over 25.0 dB insertion loss. Integrating three varactor diodes in the three-section filter created a tunable band-pass filter. The varactor-tunable filter exhibited a 20% electronic tuning range with 2.0 dB insertion loss in the passband and over 20.0 dB isolation in the stopbands.

The circuit design was based on simple transmission line models. The insertion loss of the microstrip, slotline, and CPW was included. The discontinuity effects between the slotline and coplanar resonator were not included. The parasitics of the devices were obtained from the vendor catalog,

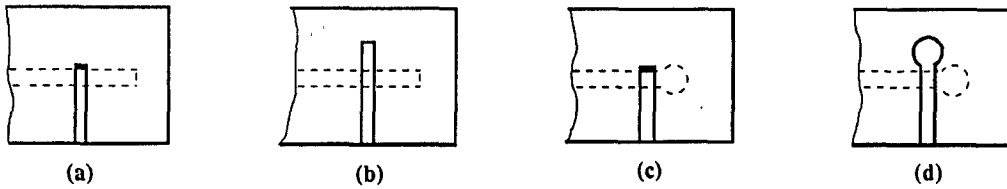
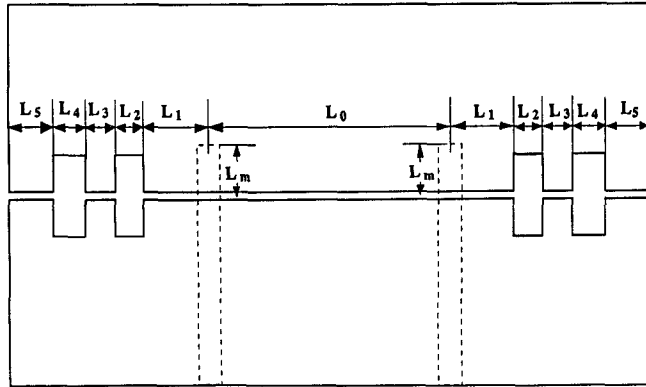
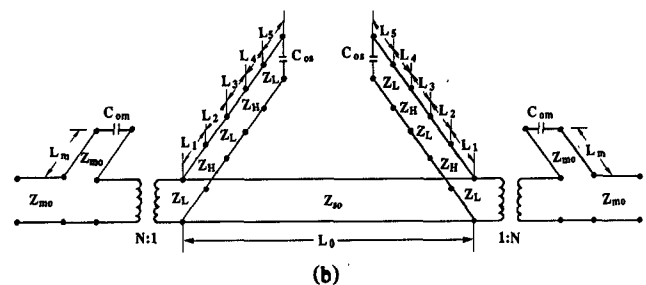


Fig. 2. Different microstrip-to-slotline transitions. (Solid line: microstrip line. Dashed line: slotline.) (a) Soldered microstrip short and uniform  $\lambda/4$  slotline. (b) Virtual short with uniform  $\lambda/4$  open microstrip and uniform  $\lambda/4$  slotline. (c) Soldered microstrip short and slotline open circuit through nonuniform circular slotline. (d) Virtual short with nonuniform circular microstrip and slotline open circuit through nonuniform circular slotline.



(a)



(b)

Fig. 3. The novel microstrip-to-slotline transition: (a) configuration; (b) equivalent circuit.

which gives typical values only. Even with these uncertainties, the analysis did predict the performance of the transitions and filters. Better agreement between theory and experiment could be achieved with more accurate information and analysis.

These new filters offer low passband insertion loss and high stopband isolation. The theoretical and experimental results agree well. These filters are amenable to monolithic implementation. The circuit configurations should have many applications in microwave and millimeter-wave systems.

## II. MICROSTRIP-TO-SLOTLINE TRANSITION

Low-loss, wide-band microstrip-to-slotline transitions have been reported in the literature. Schuppert [13] reviews the different transitions shown in Fig. 2. These transitions offer good performance and are widely used for circuit design. Owing to the requirements of device biasing, we developed a new microstrip-to-slotline transition which incorporates a dc block and a slotline low-pass filter for an RF choke.

Fig. 3(a) shows the microstrip-to-slotline transition circuit. The circuit consists of two microstrip-to-slotline transitions, two slotline low-pass filters, and two dc blocks for device biasing. Fig. 3(b) shows the equivalent circuit for the transi-

tion.  $C_{om}$  and  $C_{os}$  represent the open circuit capacitance for microstrip and slotline, respectively. The transmission line characteristic impedance of microstrip and slotline are defined by  $Z_{m0}$  and  $Z_{s0}$ , respectively.  $Z_{m0}$  is equal to  $50 \Omega$  while  $Z_{s0}$  is equal to  $60 \Omega$ , respectively.  $Z_L$  and  $Z_H$  are the low and high impedance values used in the slotline low-pass filter design, respectively. The transformer ratio,  $N$ , is reported by [14] to be

$$N = \frac{V(h)}{V_0} \quad (1)$$

where

$$V(h) = - \int_{-b/2}^{b/2} E_y(h) dy \quad (2)$$

where  $h$  is the thickness of the substrate,  $b/2$  is the length of the microstrip feed to the slotline,  $V_0$  is the voltage across the slot, and  $E_y(h)$  is the electric field of the slotline on the dielectric surface on the opposite side. From Cohn's analysis [15],

$$E_y(h) = - \frac{V_0}{b} \left( \cos \left( \frac{2\pi U}{\lambda_0} h \right) - \cot(q_0) \sin \left( \frac{2\pi U}{\lambda_0} h \right) \right) \quad (3)$$

where

$$q_0 = \frac{2\pi U}{\lambda_0} h + \arctan \left( \frac{U}{V} \right) \quad (4)$$

$$U = \sqrt{\epsilon_r - \left( \frac{\lambda_0}{\lambda_{gs}} \right)^2} \quad (5)$$

$$V = \sqrt{\left( \frac{\lambda_0}{\lambda_{gs}} \right)^2 - 1} \quad (6)$$

where  $\lambda_{gs}$  is the guided wavelength of the slotline.

A computer program based on the equivalent circuit of Fig. 3(b) was developed and used to analyze and optimize the transition's performance. The lengths of the microstrip open stubs ( $L_m$ ), each section of the slotline low-pass filter ( $L_1, L_2, L_3, L_4, L_5$ ) and interconnecting slotlines ( $L_0$ ) were optimized at fixed characteristic impedance values for the required reflection ( $S_{11}$ ) and insertion ( $S_{21}$ ) characteristics. The program was optimized for maximum insertion loss ( $S_{21}$ ) of  $-0.5$  dB with a minimum return loss ( $S_{11}$ ) of  $-20$  dB throughout the 2.0 to 4.0 GHz range. Closed-form equations for microstrip [16], [17] and slotline [18] transmission lines were used to analyze the circuit parameters. The transitions were fabricated on a 50-mil-thick RT-Duroid 6010.5 sub-

TABLE I  
OPTIMIZED LENGTHS OF TRANSMISSION LINES OF  
MICROSTRIP-TO-SLOTLINE  
TRANSITION SHOWN IN FIG. 3(a)  
 $Z_H = 245 \Omega$ ,  $Z_L = 60 \Omega$ ,  $Z_{m0} = 50 \Omega$ ,  $Z_{s0} = 60 \Omega$

Variable	$L_0$	$L_1$	$L_2$	$L_3$	$L_4$	$L_5$	$L_m$
mm	26.70	4.90	0.90	0.76	2.53	15.90	9.70

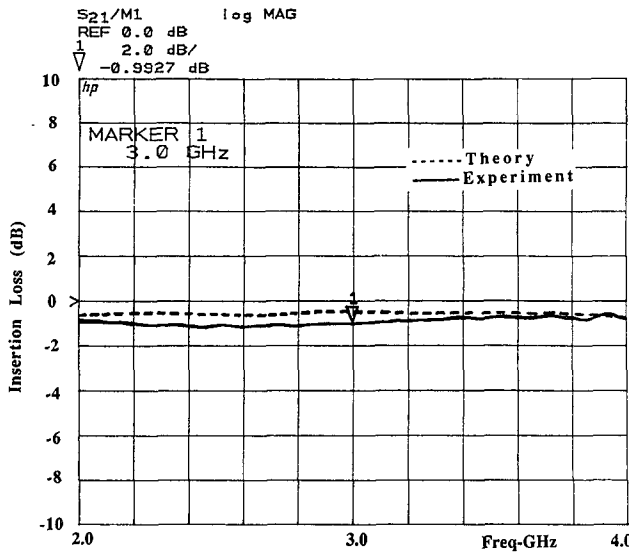


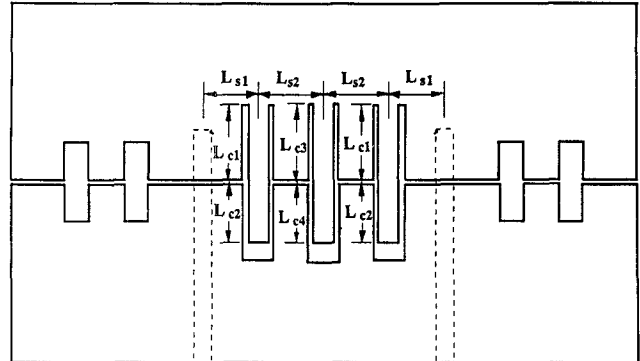
Fig. 4. Theoretical and experimental insertion loss of the transition.

strate and the  $S$  parameters were tested using standard SMA connectors with an HP-8510 network analyzer. Table I lists the optimized circuit dimensions and Fig. 4 shows the theoretical and experimental insertion loss of the transitions, respectively. The experimental insertion loss of two transitions is less than 1.0 dB in the 2.0 to 4.0 GHz frequency range. This loss performance is considered very good since it includes two coaxial-to-microstrip transitions, two microstrip-to-slotline transitions, and a 26 mm length of slotline. Overall, the theoretical and experimental results agree well. This circuit was used to test the CPW-slotline filters.

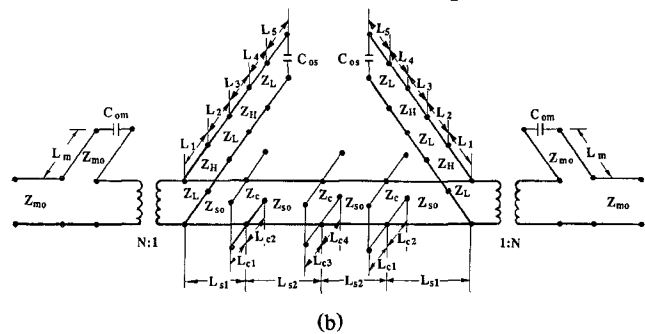
### III. THE CPW-SLOTLINE BAND-PASS FILTERS

Fig. 1 shows a cross-sectional view of the CPW transmission line. CPW allows the easy integration of series and shunt devices on a planar transmission line. Previous CPW band-pass filters [1] used end-coupled resonators. Although these circuits show good performance, device mounting and biasing are difficult to incorporate. This section describes the use of CPW resonators coupled via slotlines to create a new CPW-slotline band-pass filter.

The most basic design element of a band-pass filter is the resonator. Resonators can be designed with a combination of open and short terminations. Because of the ease of device integration, our filter uses CPW resonators with an open and a shorted end interconnected via slotline. Fig. 5 shows the novel CPW-slotline band-pass filter configuration and its equivalent circuit. The microstrip-to-slotline transition is used to test the filter. The insertion loss through a pair of transitions is about 1.0 dB across the 2.0 to 4.0 GHz range, as described in Section II.



(a)



(b)

Fig. 5. The novel CPW-slotline band-pass filter: (a) configuration; (b) equivalent circuit.

TABLE II  
OPTIMIZED LINE LENGTHS OF CPW-SLOTLINE BAND-PASS FILTER  
SHOWN IN FIG. 5  
 $Z_H = 245 \Omega$ ,  $Z_L = 60 \Omega$ ,  $Z_{m0} = 50 \Omega$ ,  $Z_{s0} = 60 \Omega$ ,  $Z_c = 50 \Omega$

Variable	$L_{c1}$	$L_{c2}$	$L_{c3}$	$L_{c4}$	$L_{s1}$	$L_{s2}$
mm	18.70	16.23	18.26	17.00	3.00	10.35

From the equivalent circuit, a computer model using cascading transmission lines was developed. The model accounts for all open and short termination effects. The model optimized the CPW resonators and interconnecting slotline lengths to achieve at least 30.0 dB insertion loss in the stopbands (2.0–2.5; 3.3–4.0 GHz) and less than 0.2 dB in the passband (2.75–3.05 GHz). The closed-form equations for CPW in [18] were used to analyze the circuit parameters. The characteristic impedances of the CPW resonators and interconnecting slotlines are 50  $\Omega$  and 60  $\Omega$ , respectively. To minimize optimization variables and form a symmetrical configuration, the lengths of the first and third resonators are equal to each other. The optimization variables  $L_{s1}$ ,  $L_{s2}$ ,  $L_{c1}$ ,  $L_{c2}$ ,  $L_{c3}$  and  $L_{c4}$  are shown in Fig. 5 and the optimized dimensions are given in Table II.

The filter and transitions were fabricated on a 50-mil-thick RT-Duroid 6010.5 substrate and the  $S$  parameters were measured using standard SMA connectors with an HP-8510 network analyzer. Fig. 6 shows the theoretical and experimental insertion loss of the filter with the transitions, respectively. In the passband, the theoretical insertion loss (including transition loss) is around 0.7 dB at a center frequency of 2.9 GHz. The experimental results of the CPW-slotline filter with two microstrip-to-slotline transitions show a center fre-

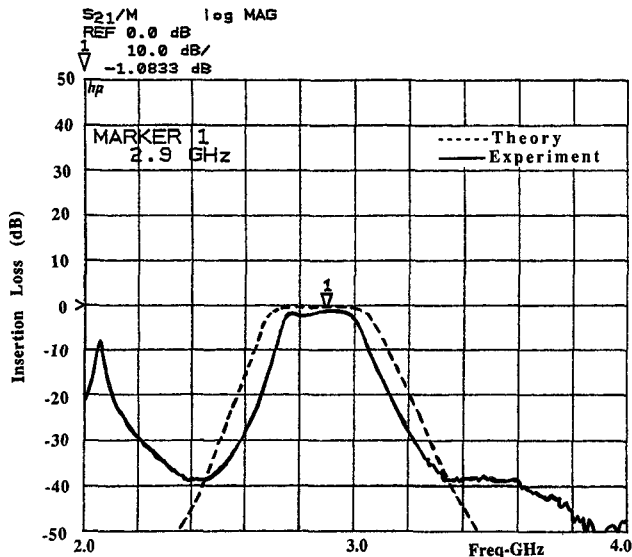


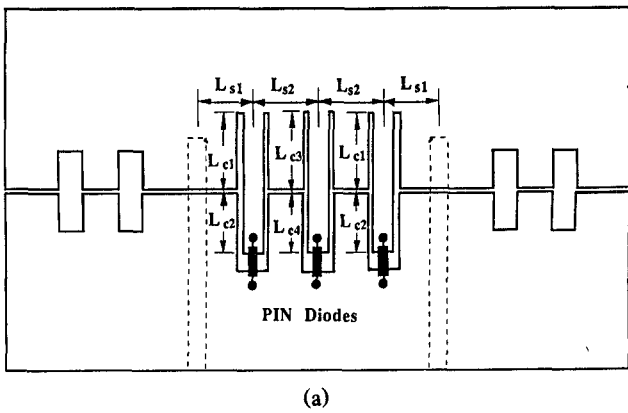
Fig. 6. Theoretical and experimental insertion loss of the novel CPW-slotline band-pass filter.

quency of 2.9 GHz with an insertion loss of less than 1.2 dB. The actual loss due to filter excluding the transition loss is only 0.2 dB. The stopband isolation is greater than 30.0 dB except for a microstrip feedline stub resonance from the transition at 2.1 GHz. The feedline resonance is due to the quarter-wavelength stub ( $L_m$  in Fig. 3(a)) resonating at 2.1 GHz. The effect could be eliminated by using a  $\frac{3}{4}\lambda$  stub. The stub resonance was verified using the HP-8510 time-domain functions. The filter was isolated to show that the spike at 2.1 GHz was not due to the filter. The theoretical model generally predicts the experimental performance. The design can be easily modified for different frequencies and passband characteristics.

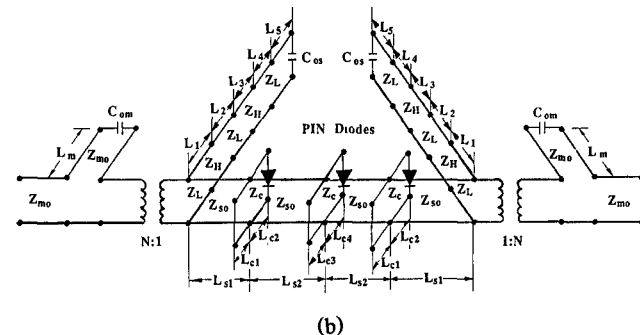
#### IV. P-I-N DIODE SWITCHABLE CPW SLOTLINE BAND-PASS FILTERS

Switchable band-pass filters have many applications in microwave systems. Martin *et al.* [19] integrated p-i-n diodes into a ring resonator to form a switchable ring resonator. This section describes the integration of p-i-n diodes into the planar CPW-slotline filter to create a switchable microwave filter. The p-i-n diodes are mounted over the open end of the CPW resonators. Fig. 7 shows the circuit configuration and equivalent circuit of the three-section, three-diode switchable filter. The p-i-n diode has the equivalent circuit shown in Fig. 8.  $R_f$  is the forward-biased series resistance of the diode while  $R_r$  is the reversed-biased series resistance.  $C_j$  represents the junction capacitance and  $L_p$  and  $C_p$  represent the package parasitics.  $L_s$  accounts for the inductance of the bonding wire to the semiconductor material in the diode. The p-i-n diodes used are M/A COM 47047's with  $L_p = 2.0 \text{ nH}$ ,  $C_p = 0.1 \text{ pF}$ ,  $L_s = 0.2 \text{ nH}$ , and  $C_j = 0.3 \text{ pF}$  at  $-50 \text{ V}$  and  $R_f = 1.3 \Omega$  at 100 mA. Although  $R_r$  is not quoted, similar reversed-biased devices show a resistance of  $2 \Omega$ . These values were used in the computer model analysis and optimization.

In the design procedure, while the p-i-n diodes are reversed-biased (OFF state), the lengths of the resonators and



(a)



(b)

Fig. 7. The p-i-n diode switchable CPW-slotline band-pass filter: (a) configuration; (b) equivalent circuit.

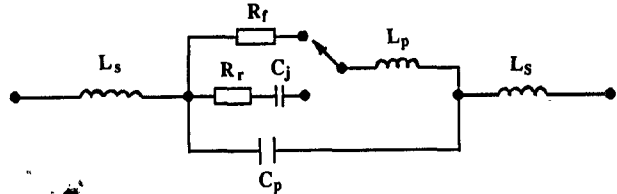


Fig. 8. The equivalent circuit of a p-i-n diode.

TABLE III  
OPTIMIZED LENGTHS OF THE THREE-SECTION, THREE-P-I-N DIODE  
SWITCHABLE CPW-SLOTLINE BAND-PASS FILTER  
SHOWN IN FIG. 7

Variable	$L_{c1}$	$L_{c2}$	$L_{c3}$	$L_{c4}$	$L_{s1}$	$L_{s2}$
mm	19.99	15.45	19.93	12.19	3.18	9.23

interconnecting lines are optimized to provide low insertion loss in the passband and high rejection in the stopbands. The p-i-n diodes are then forward-biased (ON state) to determine if the circuit meets the isolation specification across the whole band. The circuit was optimized for minimum insertion loss in the passband when the p-i-n diodes are reversed-biased and maximum isolation when the p-i-n diodes are forward-biased.

Table III shows the circuit dimensions for the switchable filter. The switchable filter was fabricated on a 50-mil-thick RT-Duroid 6010.5 substrate and the  $S$  parameters were tested using standard SMA connectors with an HP-8510 network analyzer. Fig. 9 shows the theoretical and experi-

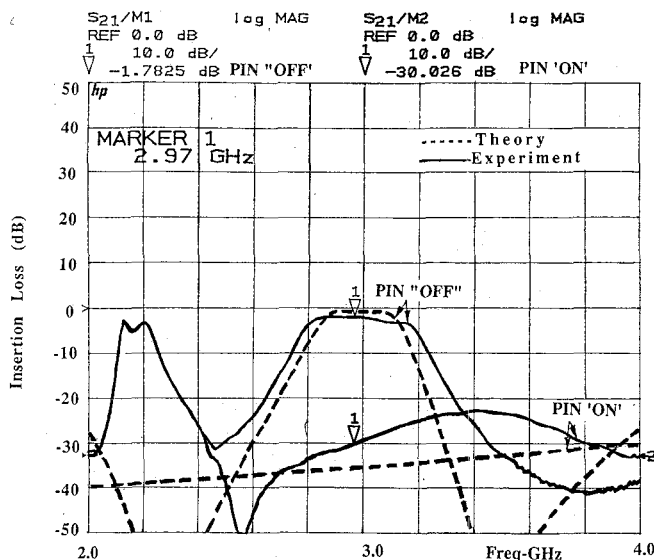


Fig. 9. The theoretical and experimental results of the p-i-n diode switchable band-pass filter.

mental results of the switchable filter. From the theoretical results, the center frequency is 3.0 GHz with an insertion loss (including the transition loss) of 1.0 dB when the p-i-n diodes are OFF. When the p-i-n diodes are ON, the isolation is at least 30.0 dB across the 2.0 to 4.0 GHz range. The experimental results indicated an insertion loss of 1.7 dB in the passband and over 25.0 dB isolation except for a spike at 2.1 GHz. The reasons for the spike are explained in Section III. This loss includes the 1.0 dB loss caused by the two transitions; therefore, the actual filter loss is only 0.7 dB.

This planar integrated circuit can be easily assembled at very low cost. The good switching performance has many system applications. Because of the planar nature, this circuit is amenable to monolithic implementation.

## V. VARACTOR-TUNABLE CPW-SLOTLINE BAND-PASS FILTERS

Electronically tunable microwave filters have many applications in a wide range of microwave systems which require broad tuning ranges and fast tuning speed. Although YIG-tuned filters offer very wide tuning ranges, they are limited in tuning speed. Varactors can provide wide tuning ranges with high tuning speed for frequency agile systems. Hunter and Rhodes [20] have developed varactor-tunable combine filters, while Makimoto and Sagawa [21] have developed varactor-tunable microstrip ring filters. This section describes the integration of three varactors with the CPW-slotline filter to create a varactor-tunable band-pass filter. The varactors are mounted over the open end of the CPW resonator in the same manner as the p-i-n diodes of the switchable filter. Fig. 10 shows a photograph of the varactor-tunable CPW-slotline filter. The circuit configuration and equivalent circuit are the same as in Fig. 7, except that the p-i-n diodes are replaced by varactor diodes. The varactor equivalent circuit used in the circuit model is shown in Fig. 11.  $R_s$  is the series resistance of the diode while  $C_p$  represents the package capacitance.  $L_s$  accounts for the inductance of the bonding wire to the package. The junction capacitance,  $C_j(V)$ , varies as a function of bias voltage from

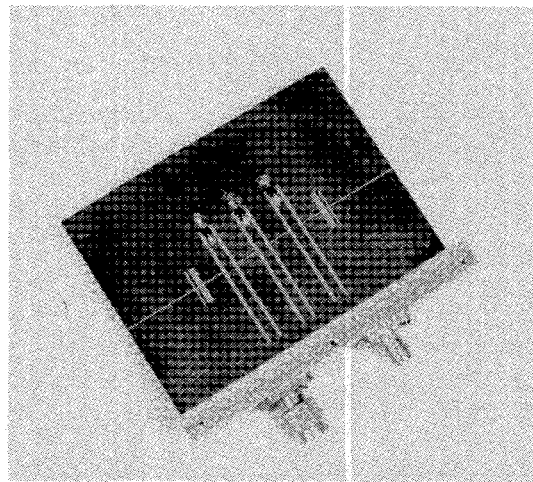


Fig. 10. A photograph of the varactor-tunable CPW-slotline band-pass filter.

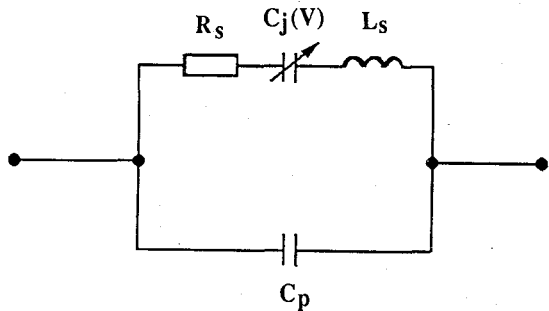


Fig. 11. The equivalent circuit of a varactor diode.

0 to 30 V. The varactor diodes used are from M/A COM (model 46600) with  $L_s = 0.2 \text{ nH}$ ,  $C_p = 0.25 \text{ pF}$ , and  $R_s = 8 \Omega$ .  $C_j$  varies from 0.5 to 2.5 pF. These approximate values were used to optimize the circuit parameters in the model. The junction capacitance used in the circuit optimization was 1.0 pF. The center frequency for the design optimization was set at 3.0 GHz with a  $\pm 200 \text{ MHz}$  bandwidth. The circuit model optimized the passband to less than 1.5 dB insertion loss with more than 30.0 dB isolation in the stopbands.

Table IV shows the optimized circuit dimensions for the varactor-tunable filter. The varactor-tunable filter was fabricated on a 50-mil-thick RT-Duroid 6010.5 substrate. Parts (a) and (b) of Fig. 12 show the theoretical and experimental results of the varactor-tunable filter. The frequency tuning range agrees well but there is a discrepancy in the bandwidth. The theoretical bandwidth increases at the lower end while the experiment shows an increase at the higher end. This discrepancy could be due to the simplified model used in the analysis. The model does not account for discontinuities of the CPW to slotline junctions, the variation of the  $Q$  factor of the varactor as a function of voltage, and the variation of the device parasitics.

A tuning bandwidth of 600 MHz was achieved for varactor bias voltages of 0 to 25 V. The maximum insertion loss of 2.15 dB (excluding the 1.0 dB transition loss) occurs at the low-end frequency of 2.7 GHz and decreases to 0.7 dB at the high-end frequency of 3.3 GHz. The passband varies from 250 MHz in the low end to 450 MHz in the high end.

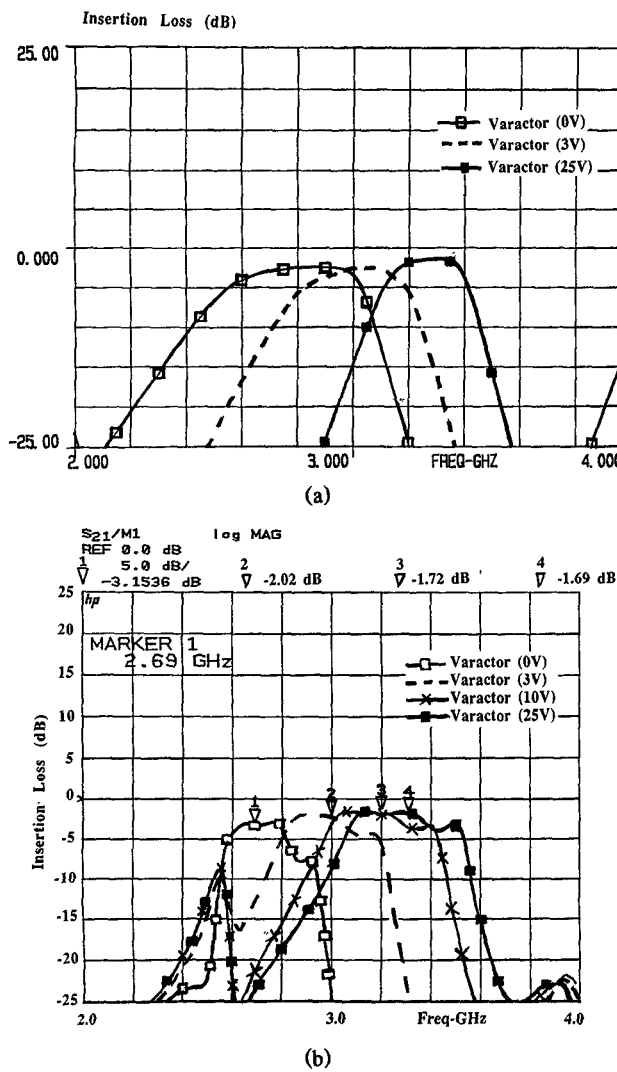


Fig. 12. The varactor-tunable CPW-slotline band-pass filter: (a) theoretical insertion loss; (b) experimental insertion loss.

TABLE IV OPTIMIZED LENGTHS OF THE VARACTOR-TUNABLE CPW-SLOTLINE BAND-PASS FILTER SHOWN IN FIG. 7 WITH P-I-N -DIODES REPLACED BY VARACTOR DIODES						
Variable	$L_{c1}$	$L_{c2}$	$L_{c3}$	$L_{c4}$	$L_{s1}$	$L_{s2}$
mm	19.57	8.84	19.99	8.59	3.20	9.03

Unequal passbands have been reported before for other types of varactor-tuned filters [21].

## VI. CONCLUSIONS

Novel CPW-slotline band-pass filters and microstrip-to-slotline transitions have been developed. Two transitions incorporating dc blocks and three-section slotline low-pass filters were designed to achieve 1.0 dB insertion loss over the 2.0 to 4.0 GHz range. A novel band-pass filter was developed using three coplanar waveguide resonators cascaded by slotlines. The filters were made switchable and tunable by incorporating the p-i-n and varactor diodes in the resonators, respectively. Wide-band switching and tuning were achieved

with low insertion loss in the passband and high isolation in the stopbands.

A simple CAD model and a computer program have been developed to optimize the various parameters for the required filter design. These circuits offer many advantages, among them low cost, low loss, high isolation, and ease of series and shunt device integration. The filters have many applications in various microwave systems. The circuits are amenable to monolithic circuit integration and can be scaled to the millimeter-wave frequency range.

## ACKNOWLEDGMENT

The authors would like to thank R. C. Waits for his instruction and use of the fabrication facilities.

## REFERENCES

- [1] M. Houdart, "Coplanar lines: Application to broadband microwave integrated circuits," in *Proc. Sixth European Microwave Conf.*, 1976, pp. 49-53.
- [2] R. A. Pucel, "Design considerations for monolithic microwave circuits," *IEEE Trans. Microwave Theory Tech.*, vol. MTT-29, pp. 513-534, June 1981.
- [3] D. R. Chen and D. R. Decker, "MMIC's—The next generation of microwave components," *Microwave J.*, pp. 67-68, May 1980.
- [4] Y. Fujiki *et al.*, "Higher-order modes in coplanar-type transmission lines," *Electron. and Commun. Japan*, vol. 58-B, pp. 74-80, 1975.
- [5] T. Hatsuda, "Computation of coplanar-type stripline characteristics by relaxation method and its application to microwave circuits," *IEEE Trans. Microwave Theory Tech.*, vol. MTT-23, pp. 795-802, Oct. 1975.
- [6] J. B. Knorr and B. Kuchler, "Analysis of coupled slots and coplanar strips on dielectric substrates," *IEEE Trans. Microwave Theory Tech.*, vol. MTT-23, pp. 541-548, July 1975.
- [7] C. P. Wen, "Coplanar-waveguide directional couplers," *IEEE Trans. Microwave Theory Tech.*, vol. MTT-18, pp. 318-332, June 1970.
- [8] D. F. Williams and S. E. Schwarz, "A planar subharmonically-pumped 71 GHz receiver with integral feed antenna," *Int. J. Infrared and Millimeter Waves*, vol. 7, no. 2, pp. 183-195, 1986.
- [9] L. Yuan, J. Paul, and P. Yen, "140 GHz quasi-optical planar mixer," in *IEEE MTT-S Int. Microwave Symp.*, 1982, pp. 374-375.
- [10] Y. C. Shih, L. Q. Bui, and T. Itoh, "Millimeter-wave diplexers with printed circuit elements," *IEEE Trans. Microwave Theory Tech.*, vol. MTT-33, pp. 1465-1469, Dec. 1985.
- [11] D. F. Williams and S. E. Schwarz, "Design and performance of coplanar waveguide bandpass filters," *IEEE Trans. Microwave Theory Tech.*, vol. MTT-31, pp. 558-566, July 1983.
- [12] K. C. Gupta, R. Garg, and I. J. Bahl, *Microstrip Lines and Slotlines*. Dedham, MA: Artech House, 1979, ch. 6.
- [13] B. Schuppert, "Microstrip/slotline transitions—Modeling and experimental investigation," *IEEE Trans. Microwave Theory Tech.*, vol. 36, pp. 1272-1282, Aug. 1988.
- [14] J. B. Knorr, "Slotline transitions," *IEEE Trans. Microwave Theory Tech.*, vol. MTT-22, pp. 548-554, 1974.
- [15] S. B. Cohn, "Slotline field components," *IEEE Trans. Microwave Theory Tech.*, vol. MTT-20, pp. 172-174, 1972.
- [16] E. Hammerstad and O. Jensen, "Accurate models for microstrip computer-aided design," in *IEEE MTT-S Int. Microwave Symp. Dig.*, 1980, pp. 407-409.
- [17] R. Garg and K. C. Gupta, "Expressions for wavelength and impedance of slotline," *IEEE Trans. Microwave Theory Tech.*, vol. MTT-24, p. 532, 1976.
- [18] G. Ghinoi and C. Naldi, "Analytical formulas for coplanar lines in hybrid and monolithic MIC's," *Electron. Lett.*, vol. 20, no. 4, pp. 179-187, 16 Feb. 1984.
- [19] T. S. Martin, F. Wang, and K. Chang, "Theoretical and experimental investigation of varactor-tuned switchable microstrip

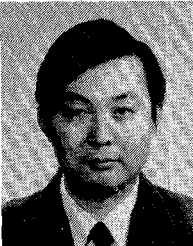
ring resonator circuits," *IEEE Trans. Microwave Theory Tech.*, vol. 36, pp. 1733-1740, Dec. 1988.

[20] I. C. Hunter and J. D. Rhodes, "Electrically tunable microwave bandpass filters," *IEEE Trans. Microwave Theory Tech.*, vol. MTT-30, pp. 1354-1360, Sept. 1982.

[21] M. Makimoto and M. Sagawa, "Varactor tuned bandpass filters using microstrip-line ring resonators," in *IEEE MTT-S Int. Microwave Symp. Dig.*, 1986, pp. 411-414.

✉

✉



**Yong-Hui Shu** was born in Jiangsu, China, on April 24, 1957. He received the B.S. and M.S. degrees in electrical engineering from the Nanjing Institute of Technology, Nanjing, China in 1982 and 1985, respectively.

From March 1985 to July 1989, he was with the Department of Radio Engineering of Nanjing Institute of Technology (current name, Southeast University) as a Lecturer. From August 1989 to July 1990, he was with the Department of Electrical Engineering of Texas A&M University as a Research Associate. In August 1990, he joined Epsilon Lambda Electronics Corporation, Geneva, IL, as a Microwave Design Engineer. His current interests are in microwave and millimeter-wave devices, circuits, and subsystems.

Mr. Shu has published 20 technical papers in microwave and millimeter-wave areas.

✉

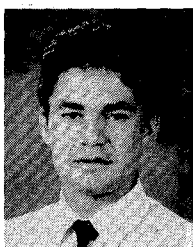
initiated projects involved with active varactor tunable end-fire radiating elements, switchable and tunable CPW filters, and varactor-tuned CPW oscillators (patents pending). He has also developed K- and Ka-band aperture-coupled patch antennas for a NASA-Lewis-Texas Instruments project. He is currently completing the requirements for the M.S.E.E. degree and will pursue Ph.D. studies under the direction of Dr. Kai Chang.



**Kai Chang** (S'75-M'76-SM'85-F'91) received the BSEE degree from the National Taiwan University, Taipei, Taiwan, the MS degree from the State University of New York at Stony Brook, and the PhD degree from the University of Michigan, Ann Arbor, in 1970, 1972, and 1976, respectively.

From 1972 to 1976, he worked for the Microwave Solid-State Circuits Group, Cooley Electronics Laboratory of the University of Michigan as a Research Assistant. From 1976 to 1978, he was with Shared Applications, Inc., Ann Arbor, where he worked on computer simulation of microwave circuits and microwave tubes. From 1978 to 1981, he was with the Electron Dynamics Division, Hughes Aircraft Company, Torrance, CA, where he was involved in the research and development of millimeter-wave solid-state devices and circuits, power combiners, oscillators, and transmitters. From 1981 to 1985, he was with TRW Electronics and Defense, Redondo Beach, CA, as a Section Head developing state-of-the-art millimeter-wave integrated circuits and subsystems including mixers, VCO's, transmitters, amplifiers, modulators, up-converters, switches, multipliers, receivers, and transceivers. He joined the Electrical Engineering Department of Texas A&M University in August 1985 as an Associate Professor and was promoted to Professor in 1988. In January 1990, he was appointed E-Systems Endowed Professor of Electrical Engineering. His current interests are in microwave and millimeter-wave devices and circuits, microwave integrated circuits, microwave optical interactions, and antennas.

Dr. Chang served as the editor of the four-volume *Handbook of Microwave and Optical Components*, published by John Wiley & Sons, Inc., in 1989 and 1990. He is the editor of *Microwave and Optical Technology Letters* and of the Wiley Book Series on Microwave and Optical Engineering. He has published over 100 technical papers and several book chapters in the areas of microwave and millimeter-wave devices and circuits. Dr. Chang received the Special Achievement Award from TRW in 1984, the Halliburton Professor Award in 1988, and the Distinguished Teaching Award in 1989 from the Texas A&M University.



**Julio A. Navarro** was born in Cordoba, Argentina, on November 13, 1964. He received the B.S.E.E. degree from Texas A&M University in May 1988. He has been a cooperative education student with General Dynamics-Fort Worth since May 1985.

He has worked in avionic systems design, advanced technology and systems engineering, field engineering, antenna systems, and radar cross section research. As a master's candidate at Texas A&M University, he has